Supplementary Information

Supplementary Figure 1

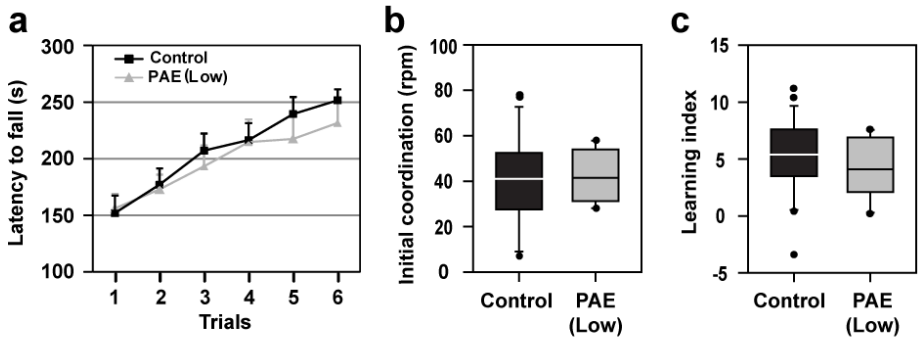

Supplementary Figure 1. Effects of PAE at a lower dose on motor skill learning. (**a**-**c**) Low-dose PAE [PAE (Low): 1.0 g/kg weight] does not show significant effects compared to control on the learning curve (**a**); F(1,33) = 0.20, P = 0.66 by two-way repeated measures ANOVA, [control: n = 25 animals, PAE (Low): n = 10 animals], initial motor coordination (at trial 1) (**b**); P = 0.77 by two-tailed Student's *t*-test [control: n = 25 animals, PAE (Low): n = 10 animals] and learning index (**c**); P = 0.30 by two-tailed Student's *t*-test [control: n = 25 animals, PAE (Low): n = 10 animals] in the accelerated rotarod test. The line graph (**a**) shows mean ± SEM. In box plots (**b**,**c**), the line within the box indicates the median, and the upper and lower edges of the box represent the 25th and 75th percentiles, respectively. The upper and lower whisker boundaries indicate the 10th and 90th percentiles, respectively, and dots indicate outliers.

Supplementary Figure 2

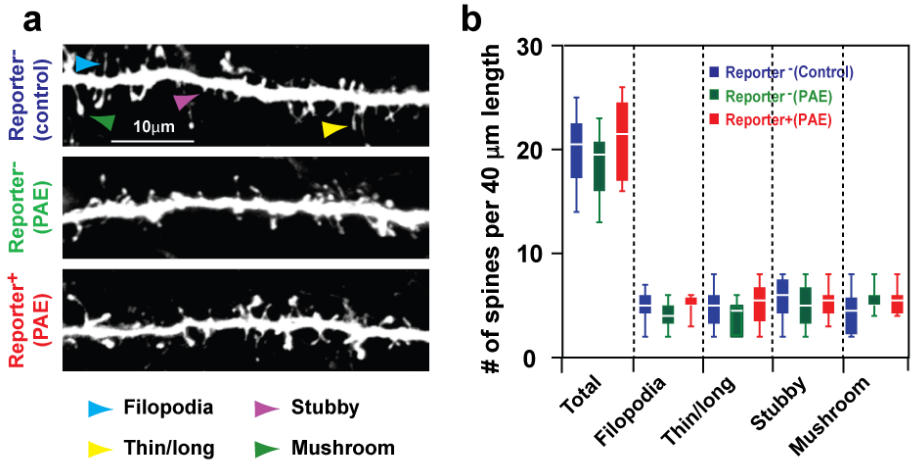

Supplementary Figure 2. Normal morphology of dendritic spines on layer III neurons in M1 in PAE mice at P30. (a) Representative images of apical dendritic spines in reporter$^-$ (control and PAE) and reporter$^+$ (PAE) neurons among electroporated neurons (n = 8 cells per group). Arrowheads in colors indicate the four morphological types of spines that were used for quantification. **(b)** There are no significant differences in the number of spines that fall in the indicated types; $F(2,21) = 0.13$, $P = 0.34$ (total spines); $F(2,21) = 1.3$, $P = 0.29$ (filopodia), $F(2,21) = 01.19$, $P = 0.32$ (thin/long); $F(2,21) = 0.23$, $P = 0.80$ (stubby), and $F(2,21) = 1.37$, $P = 0.28$ (mushroom) by one-way ANOVA. In the box plot, the line within the box indicates the median, and the upper and lower edges of the box represent the 25th and 75th percentiles, respectively. The upper and lower whisker boundaries indicate the 10th and 90th percentiles, respectively, and dots indicate outliers.

Supplementary Figure 3

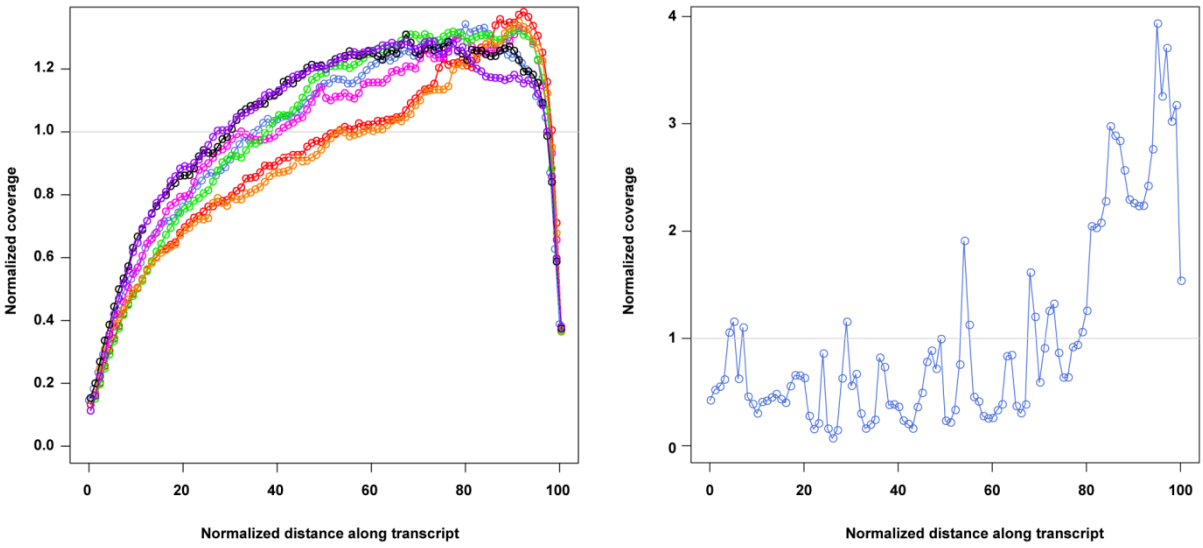

Supplementary Figure 3. Transcriptome quality. Normalized RNA-seq reads coverage was plotted across the normalized (binned) transcript length. Left: Each color pertains to a different cell. We confirmed minimum 3' bias across all transcripts. Right: A representative saw-tooth shaped plot for degraded single-cell samples. These low-quality samples were excluded from the analysis.

Supplementary Figure 4

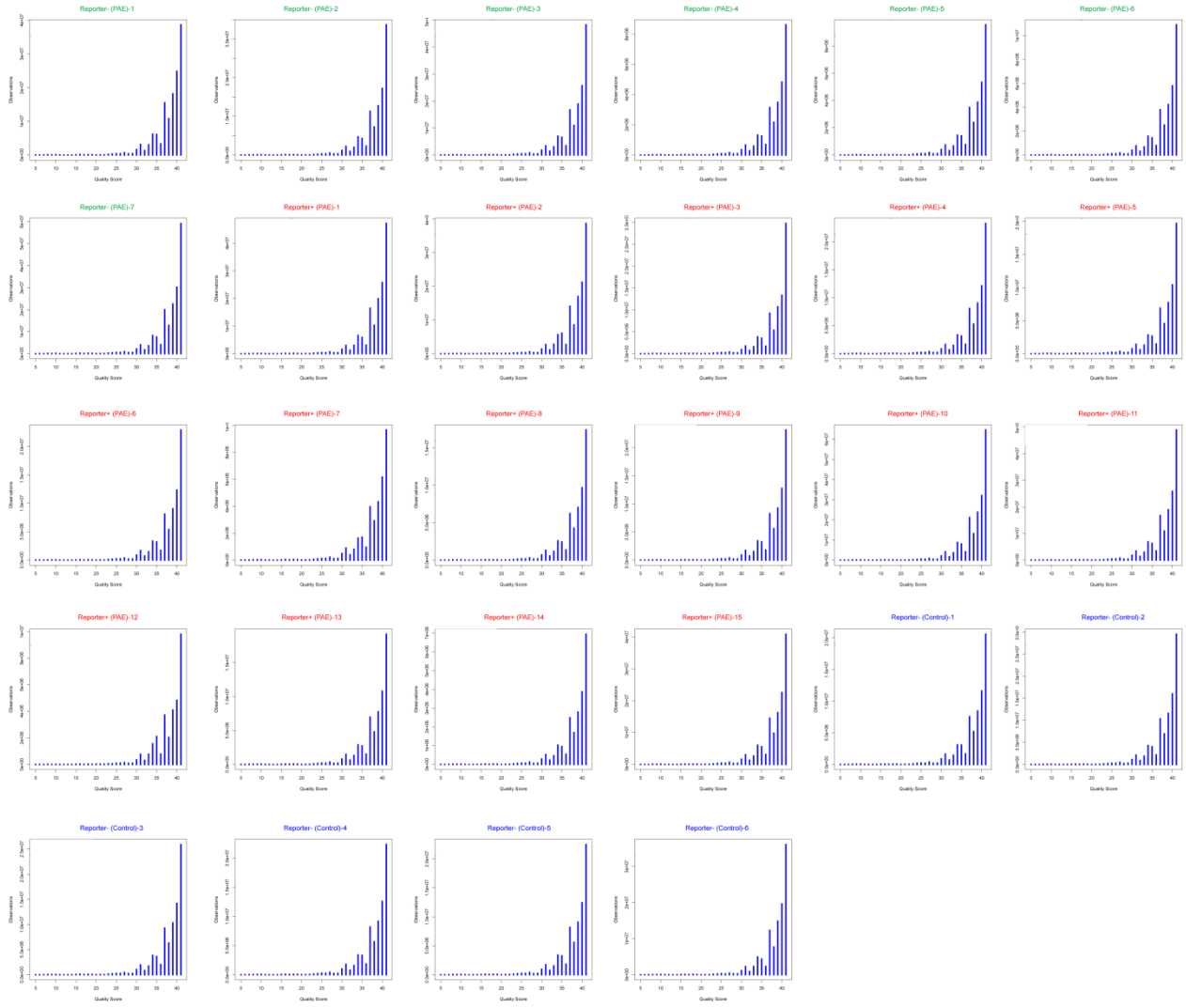

Supplementary Figure 4. Quality score distribution of the sequencing data for each single cell sample. Base calling accuracy was measured by the Phred quality score (Q score).

Supplementary Figure 5

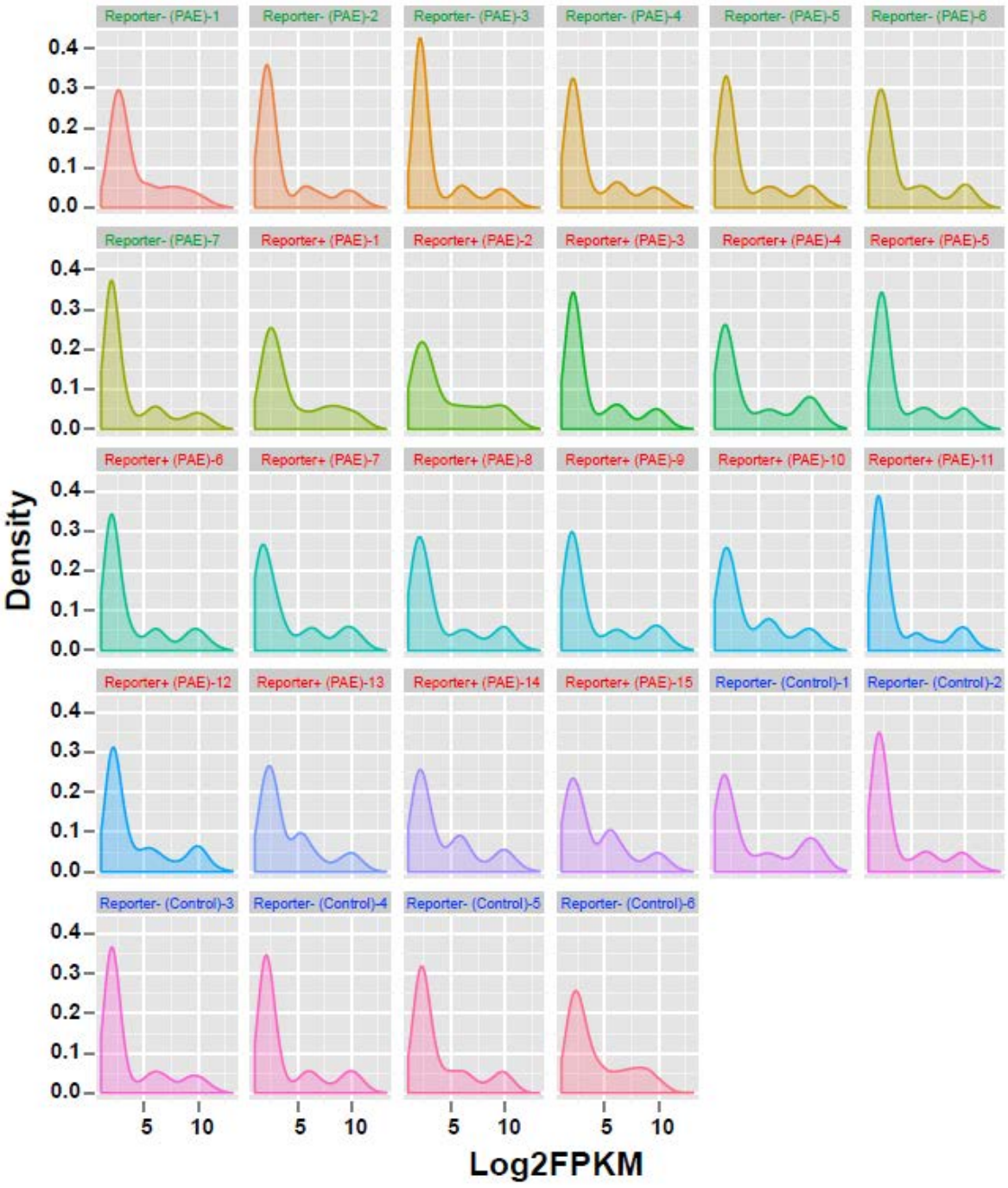

Supplementary Figure 5. Expression distribution of genes for each single cell. Each graph shows the density of quantile-normalized and log2-transformed FPKM for all annotated genes that are expressed at log2FPKM >=1 in at least one sample. The FPKM distributions are similar among all samples.

Supplementary Figure 6

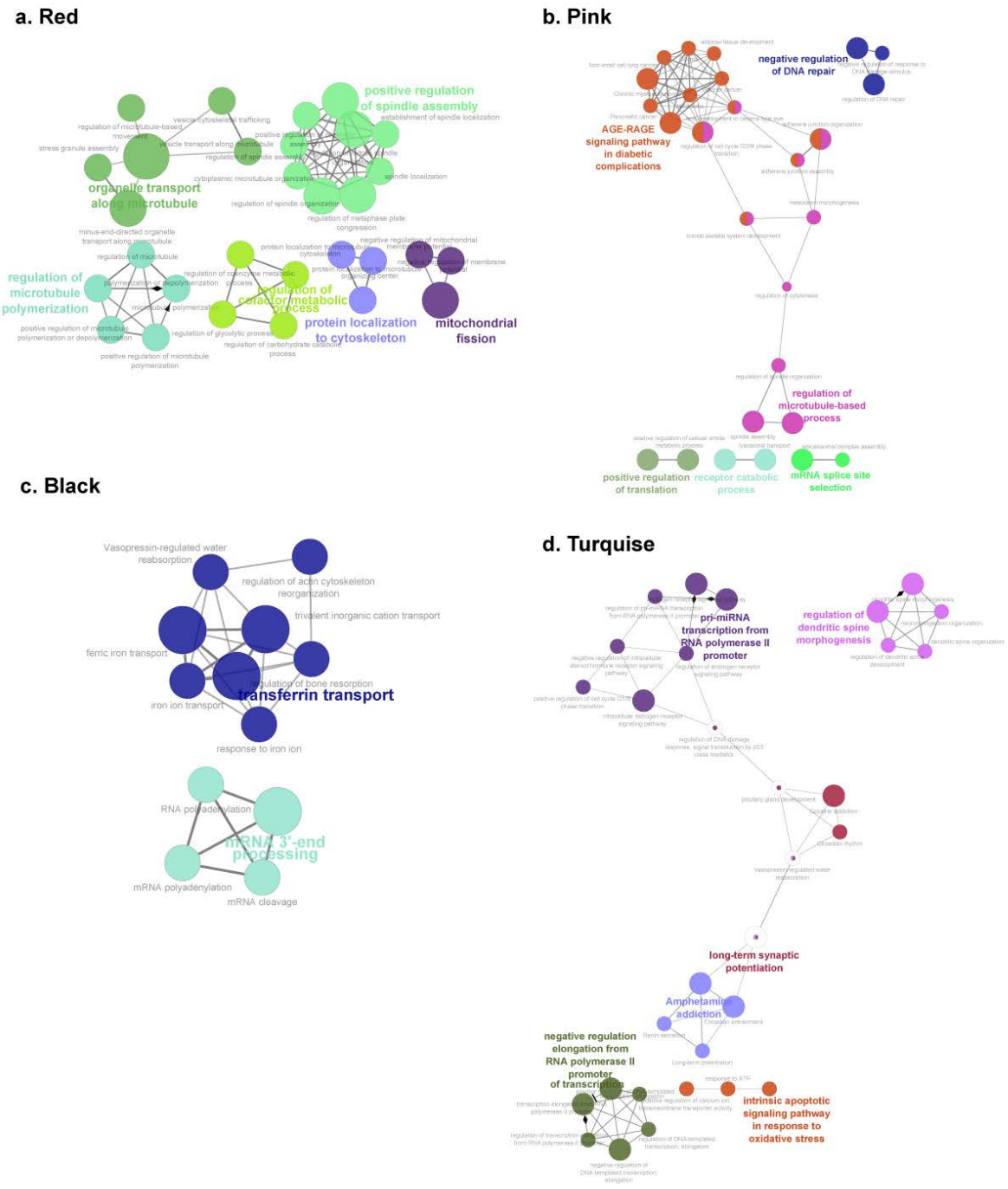

Supplementary Figure 6. GO networks of the modules that are specific to reporter- neurons. GO networks enriched in the Red (**a**), Pink (**b**), Black (**c**) and Turquoise (**d**) modules.

Supplementary Figure 7

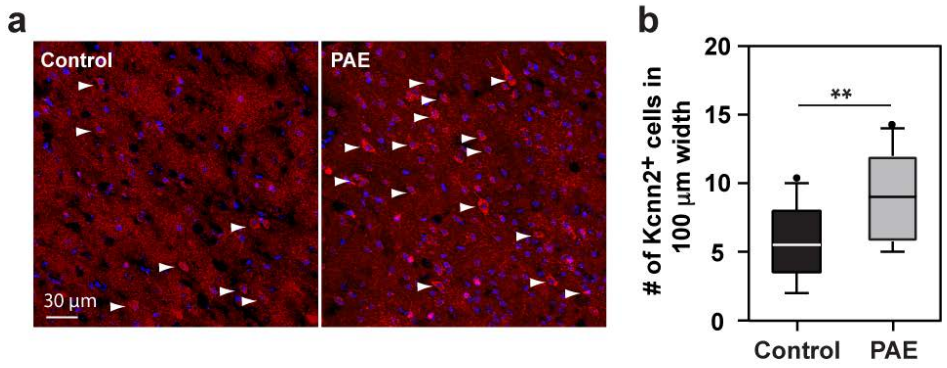

Supplementary Figure 7. Increase of Kcnn2-expressing neurons in M1 in 3-month-old PAE mice. (a) Kcnn2 immunohistochemistry in M1 of control and PAE mice at 3 months old. Arrowheads indicate $Kcnn2^+$ cells. (**b**) Quantification of $Kcnn2^+$ cells in layer III of M1, indicating significant increase of $Kcnn2^+$ cells in PAE mice. **P = 0.014 by two-tailed Student's *t*-test (n = 10 brains per group). In the box plot, the line within the box indicates the median, and the upper and lower edges of the box represent the 25th and 75th percentiles, respectively. The upper and lower whisker boundaries indicate the 10th and 90th percentiles, respectively, and dots indicate outliers.

Supplementary Figure 8

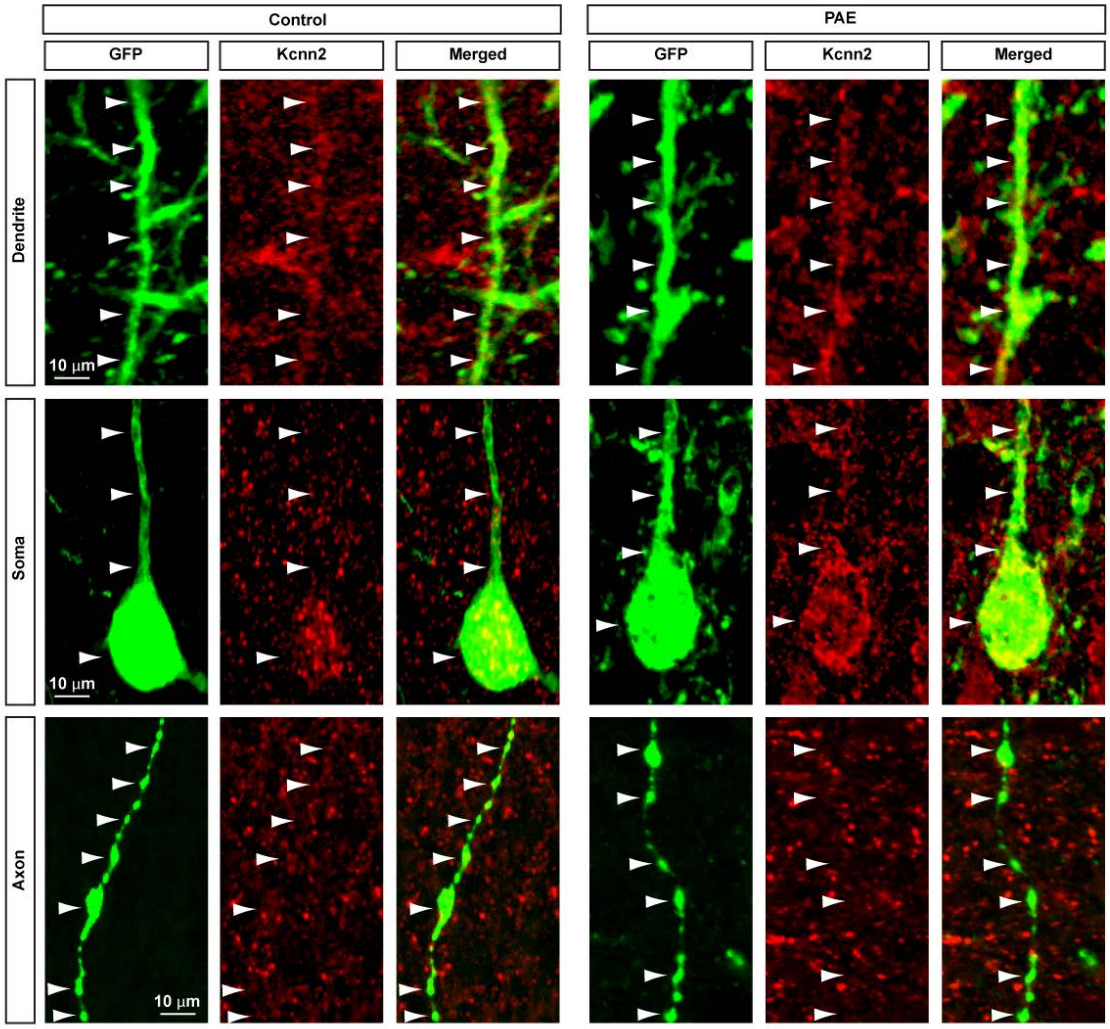

Supplementary Figure 8. Kcnn2 expression is increased in dendrites and soma of neurons. Kcnn2 immunohistochemistry at P30 in layer III of M1 in control (PBS-exposed) and PAE mice. Neurons are labeled by *in utero* electroporation with the pCAGIG plasmid at E15. Arrowheads are placed to trace the neuronal processes. $Kcnn2^{+}$ puncta that were observed in the dendrites and soma in control mice are increased in PAE mice. Labeling of Kcnn2 is not clear in axons in both control and PAE mice. Images are representatives of similar results from n = 4 animals.

Supplementary Figure 9

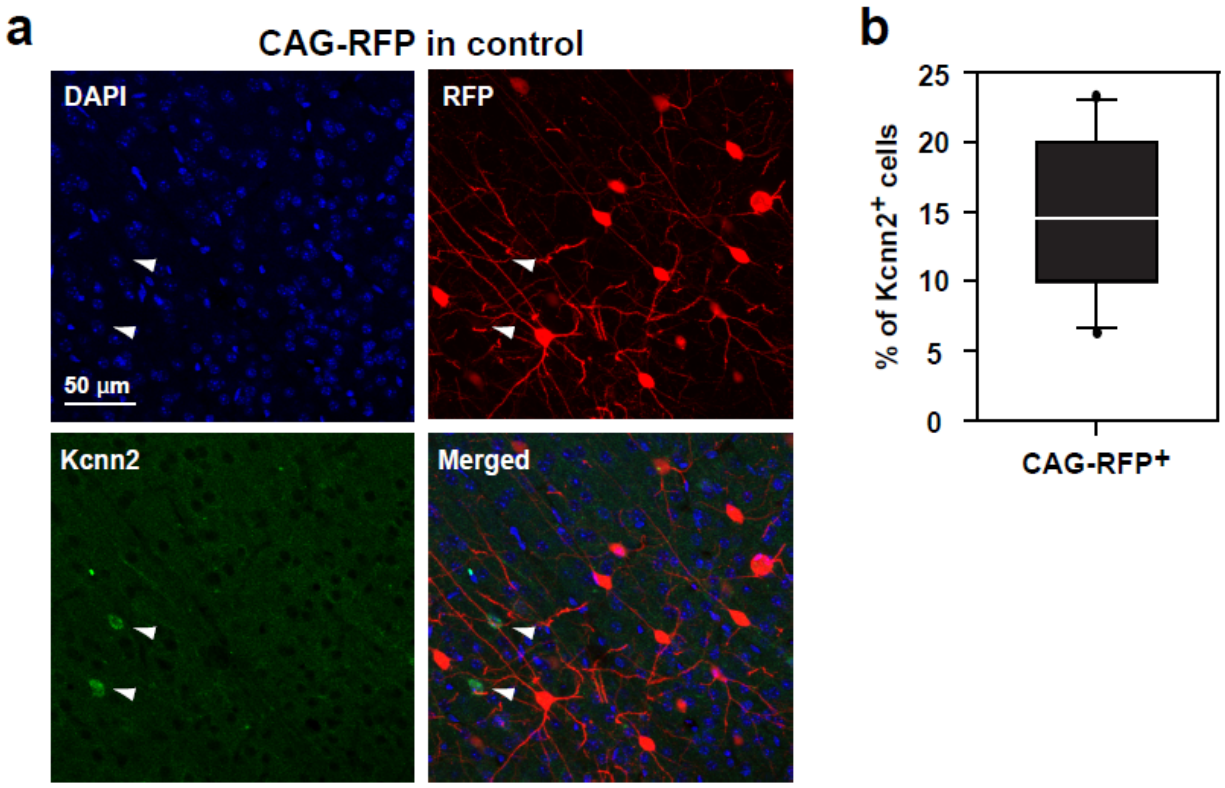

Supplementary Figure 9. RFP does not affect Kcnn2 expression. (**a**) Exogenous expression of RFP (CAG-RFP: electroporation with CAG-FLPo and FRT-RFP plasmids) per se does not increase Kcnn2 expression (green) in control (PBS-exposed) mice. Nuclei were counterstained with DAPI (blue). (**b**) The percentage of $Kcnn2^+$ neurons among RFP^+ neurons, showing no significant effect of RFP on Kcnn2 expression [compare with the data on $reporter^-$ neurons in Control mice in Fig. 4d. P = 0.16 by two-tailed Student's *t*-test (n = 10 brains per group)]. In the box plot, the line within the box indicates the median, and the upper and lower edges of the box represent the 25th and 75th percentiles, respectively. The upper and lower whisker boundaries indicate the 10th and 90th percentiles, respectively, and dots indicate outliers.

Supplementary Figure 10

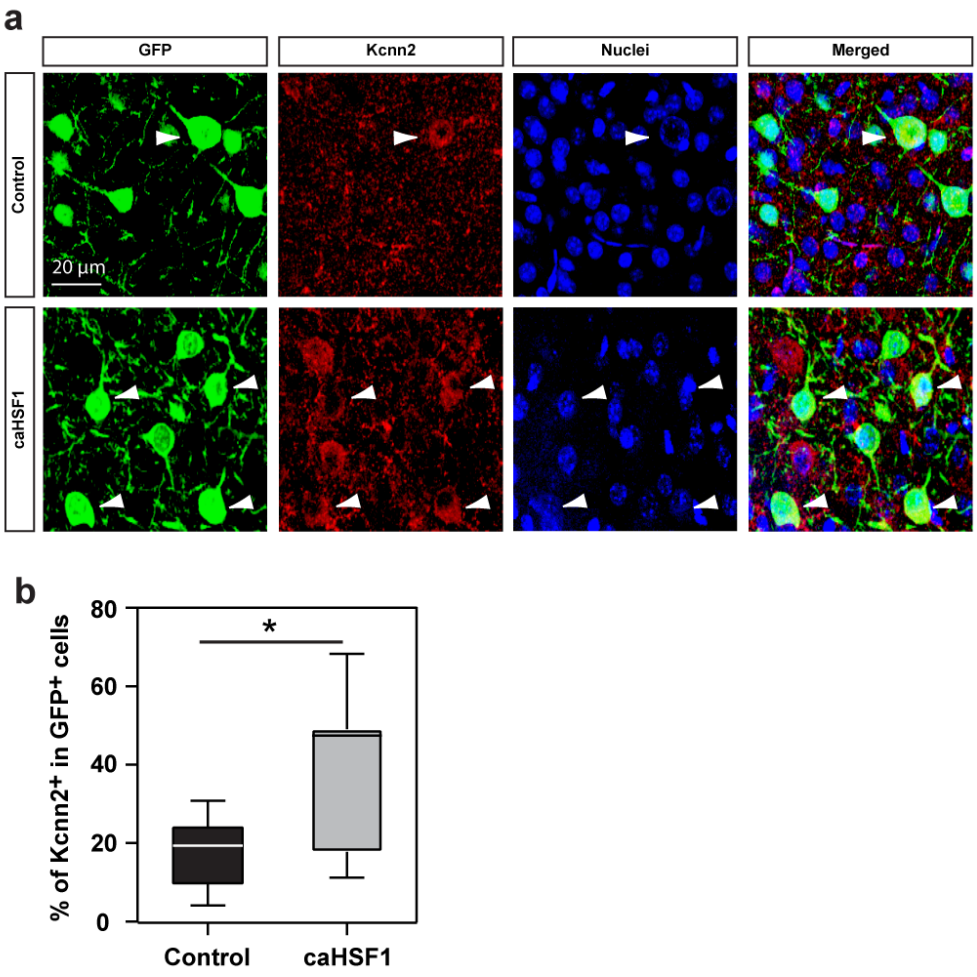

Supplementary Figure 10. Kcnn2 expression is increased by overexpression of a constitutively active form of HSF1. (**a**) The expression construct for a constitutively active form of HSF1 (caHSF1) or the control construct (empty plasmid) together with the GFP expression plasmid was transferred into M1 by *in utero* electroporation at E15, and Kcnn2 expression was detected by immunohistochemistry at P30. Kcnn2 expression (red) is increased by the expression of caHSF1. Arrowheads indicate $Kcnn2^+$ cells among GFP^+ (green) electroporated cells. (**b**) The percentage of $Kcnn2^+$ cells among GFP^+ cells is significantly increased by caHSF1 expression. P = 0.024 by two-tailed Student's *t*-test (control: n = 6 brains, caHSF1: n = 7 brains). In the box plot, the line within the box indicates the median, and the upper and lower edges of the box represent the 25th and 75th percentiles, respectively. The upper and lower whisker boundaries indicate the 10th and 90th percentiles, respectively, and dots indicate outliers.

Supplementary Figure 11

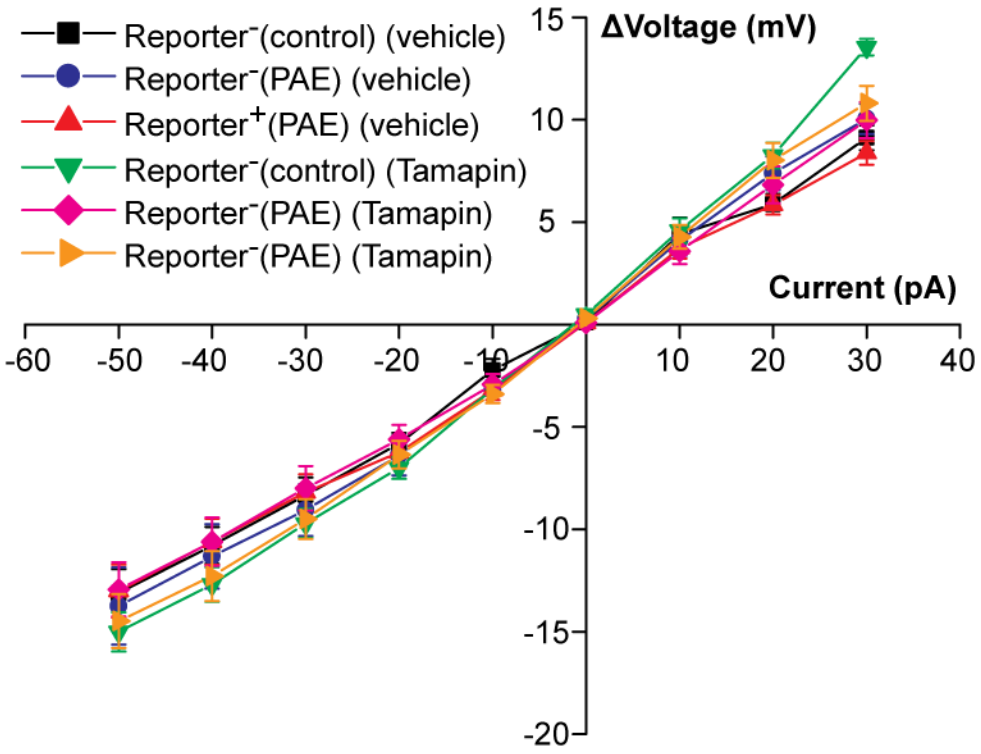

Supplementary Figure 11. Current-Voltage Relationship is not altered in PAE mice. Current-voltage relationship was plotted for reporter$^-$ neurons recorded in control and PAE mice, and reporter$^+$ neurons in PAE mice during control (aCSF) or Tamapin treatment. No differences were detected between groups; $F(1,8) = 0.72$, $P = 0.42$ by one-way repeated measures ANOVA (n = 12 cells per group). Graph shows mean ± SEM.

Supplementary Figure 12

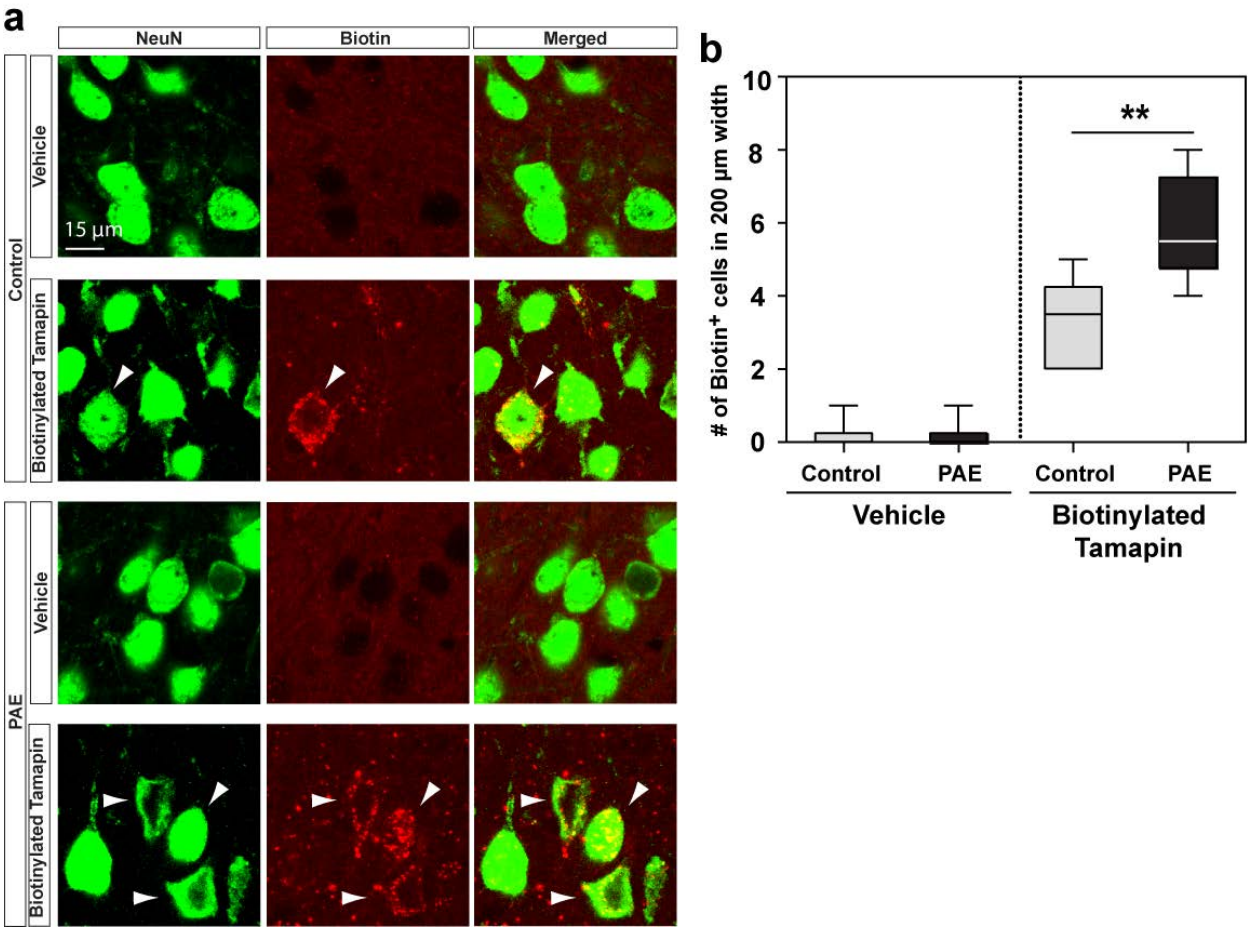

Supplementary Figure 12. Tamapin crosses the blood-brain barrier. Biotinylated Tamapin (or vehicle-only control) was injected i.p. to control and PAE mice at P30 and the cortex was labeled 30 minutes later for biotin (red) and a neuronal marker, NeuN (green). (**a**) Labeling for biotin (arrowhead) in layer III in M1 shows binding of Tamapin on a subset of neurons. (**b**) The number of neurons with Tamapin binding on the soma was increased in layer III in M1 in PAE mice compared to that in control mice; **P = 0.0093 by two-tailed Student's *t*-test (n= 6 animals per group). In the box plot, the line within the box indicates the median, and the upper and lower edges of the box represent the 25th and 75th percentiles, respectively. The upper and lower whisker boundaries indicate the 10th and 90th percentiles, respectively, and dots indicate outliers.

Supplementary Figure 13

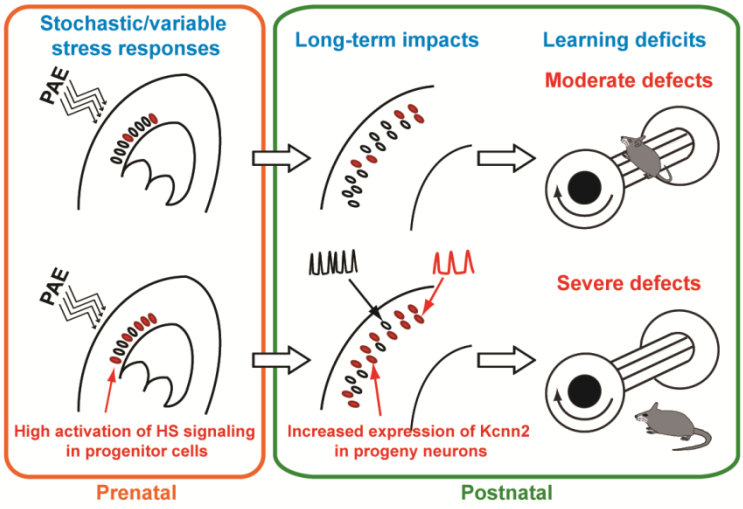

Supplementary Figure 13. A model for the emergence of variable learning deficits by prenatal exposure to alcohol. Stochastic activation of stress responses, including HS signaling activation, in cortical progenitor cells causes long-term heterogeneous impacts on gene expression, including increased Kcnn2 expression. This leads to abnormal physiological properties in neuronal progeny in the mature cortex. These molecular and physiological abnormalities at the single-cell level contribute to the deficits in learning.